Simultaneous optimization of cycle and expander design for truck on board waste heat recovery with ORC technology

Marco Manfredi, Andrea Spinelli, Marco Astolfi*

Politecnico di Milano, Energy Department, 20156, Milano, Italy

* Corresponding Author: marco.astolfi@polimi.it

ABSTRACT

Small-scale Organic Rankine Cycles (ORCs) represent a promising technology for waste heat recovery (WHR) from internal combustion engines (ICEs) for transport applications, due to their remarkable potential, especially on-board of innovative long-haul trucks. Despite market leader companies have already proved its effectiveness, detailed system design procedures are scarcely available in the open literature and proposed solutions are often more simplified with respect to current industrial state-of-art. The present work describes a methodology to include within the ORC design and optimization procedure an efficiency map of the turbo-expander, retrieved exploiting a mean line reduced-order method developed in-house. The developed ORC optimization algorithm allows to consider any working fluid in available thermodynamic databases and can investigate multiple cycle architectures. The approach proposed allows to design the thermodynamic cycle considering a realistic performance of the expander and to retrieve the best cycle architectures and turbine geometry depending on the heat source characteristic and active constraints. Methodology is applied to two WHR applications of different sizes highlighting the impact of adopting efficiency maps for the turbine within the cycle optimization procedure rather than assuming fixed efficiency values.

1. INTRODUCTION

Despite the employment of organic Rankine cycle (ORC) technology for stationary thermal recovery in the power range from 10^{-1} to 10^{-1} MW is widely spread (Tartière and Astolfi, 2017), economic and technical challenges prevent the penetration of ORCs into automotive and transportation freight sectors. However, they represent a promising solution due to the remarkable recovery potential from internal combustion engines (ICEs), which release a large fraction of the fuel energy at high-temperature through the engine hot exhaust (about 30% of the fuel inlet power) and the EGR system (about 5-10%), and at low-temperature from the charge-air cooler (about 5-10%) and the engine cooling system (about 10-15%) (Dolz et al., 2012). Despite the large market potential, design methods for onboard small-scale ORCs are not trivial requiring a meaningful working fluid selection and an optimal design and performance quantification of the thermodynamic cycle and of the small-scale components in both nominal, part load and transient conditions. For small power applications, volumetric machines are often preferred over turbo-expanders but they are constrained by limited volumetric expansion ratios (Colonna et al., 2015), making unfeasible their efficient employment in high-temperature applications. For this reason, radial inflow turbines (RITs) are usually exploited, being characterized by large power density and capability to handle high pressure ratios (PRs) within a single-stage configuration (Persico and Pini, 2017).

Despite market leader companies have already proved its effectiveness (Glensvig et al., 2016), the design procedures of bottoming ORCs available in the open literature are often more simplified with respect to current industrial state-of-art and usually adopts simplified assumptions relative to the performance of the components. In particular, the quantification of turbine efficiency during the cycle design optimization procedure is of paramount importance because of the large impact on the definition of optimal working

fluid and design parameters (e.g. maximum and minimum pressure of the cycle). In the framework of small-scale ORC design for onboard WHR, assuming a constant turbine efficiency may result into misleading optimal cycle configurations having turbine expansion ratios and dimensions non compatible with the assumed turbine efficiency, especially if the number of stages and the rotational speed are constrained by rotodynamic, available space and economic factors. Similarly, a coupled sensitivity analysis on turbine efficiency (Bademlioglu et al., 2018) results ineffective to optimize the ORC design variables, since they are only slightly affected by the specific value of the turbine efficiency. An apparently more reliable and complex iterative procedure, in which the ORC and turbine optimization routines are iteratively alternated (Meroni et al., 2018), turns out to be also inadequate, being the turbine efficiency still constant at each ORC optimization step, despite estimated with a dedicated design tool. A more reliable method would instead integrate the turbine efficiency quantification into the ORC optimization process to account for a realistic turboexpander performance as function of the inlet/outlet thermodynamic states at each ORC design iteration step. This is usually achieved through turbine reduced-order (or mean-line) models, capable of providing preliminary sizing and performance evaluation with a limited computational cost. The most rigorous method would require the implementation of a dedicated turboexpander optimization routine within the ORC cycle optimization tool, however this approach implies a non-feasible computational cost (even using mean line models) since several hundreds of turbine mean-line model evaluations should be performed at each ORC design iteration step. Alternatively, a higher-order optimization may be performed by varying concurrently the ORC design parameters and the geometric variables of the turbine model (Bahamonde et al., 2017). However, this approach may converge to local minima, due to the different effect of geometric and thermodynamic design variables on the turbine performance and may lead to suboptimal solutions since a low number of turbine and cycle optimized parameters is usually adopted in order to reduce the complexity of the numerical problem. Finally, other studies propose to exploit the turbine design tools to retrieve performance maps as a function of certain cycle-dependent non-dimensional parameters (Perdichizzi and Lozza, 1987; Astolfi and Macchi, 2015; Da Lio et al., 2017; White and Sayma, 2019).

In this work a maximum efficiency performance map for single-stage radial inflow turbines is integrated in the cycle optimization procedure, extending the analyses already carried out in the framework of axial machines (Astolfi and Macchi, 2015). This map reports the maximum RIT total-to-static efficiency η_{TS} as function of turbine Size Parameter (SP) and isentropic volume ratio (Vr) (as defined in (Astolfi and Macchi, 2015)), which include in their definition the effects of fluid properties (complexity and non-ideality) and were identified as the most adequate independent parameters from previous studies on ORC axial and radial turbines (E. Macchi, 1981; Perdichizzi and Lozza, 1987; Da Lio et al., 2017; Masi et al., 2020). Differently from the approach suggested by (White and Sayma, 2019), in which the map was retrieved by means of a scaling procedure applied to the results published by (Perdichizzi and Lozza, 1987), the map proposed in this work was obtained performing expander optimizations, aiming at maximizing η_{TS}, for a discrete number of SP and Vr values. In the proposed method the RIT optimization was carried out exploiting an in-house reduced-order model, whose details are in (Manfredi et al.), which adopts 10 design variables, including most of geometrical parameters and rotor rotational speed, and adopting several constraints, which have been included to obtain feasible RIT geometries. This represents a substantial improvement with respect to the approach of (Da Lio et al., 2017), where maps were obtained exploiting a bivariate optimization procedure based on specific speed and velocity ratio. Therefore, the map here reported defines an ultimate upper bound for the RIT efficiency. Moreover, since high-temperature small-power applications are considered, the ranges of Vr and SP investigated are substantially different from those reported in (Da Lio et al., 2017) and shifted towards higher Vr and lower SP. This is the reason why the present work analyzed converging-diverging nozzles in choking conditions, while previous studies only investigated converging-nozzle architectures (Perdichizzi and Lozza, 1987; Da Lio et al., 2017).

2. NUMERICAL TOOLS DESCRIPTION

Two numerical models have been developed and integrated for this study: the first one deals with the ORC cycle optimization while the second one concerns the design and optimization of single-stage radial inflow turbines and will be used for the development of the map of maximum turbine performance. Both models are implemented in Python and adopt CoolProp (Bell et al., 2014) for the calculation of fluid thermodynamic properties recalling the NIST REFPROP backend (Lemmon et al., 2018).

2.1 ORC Numerical tool description ad assumptions

The numerical code developed for on-board WHR with ORC power systems implements several features that make it a flexible tool for system optimization and technoeconomic analysis. However, the potential of the code is not fully exploited in this work according to the scope of this paper which is to investigate the strong link between turbine performance and cycle design rather than determining the optimal working fluid and cycle architecture among several different options. Despite the numerical code can analyze ORC systems integrated with multiple thermal power inputs, a single heat source is considered, namely the engine exhaust. MAN D2676 (Yang et al., 2018), with 316 kW nominal brake power output at 1800 rpm, is selected as reference engine and exhaust reference thermodynamic conditions are obtained at 50% of the engine load. In this condition, the hot exhaust stream, modelled as ideal gas with constant specific heat (1.035 kJ/kgK), has mass flow rate equal to 0.2 kg/s and temperature at the primary heat exchanger (PRHE) inlet equal to 351°C. The developed numerical code can deal with any fluid available in RefProp database but the analyses are carried out considering the hydro-fluoro-olefin R1233zd(E) only. Such fluid was selected as environmentally friendly drop-in substitute fluid for R245fa with extremely low ODP, very small GWP, and low safety issues, and therefore widely suggested as a promising candidate for automotive climatization as it is compatible with present and future regulation (Committee, 2020). A single pressure level cycle is selected in both subcritical and supercritical configurations, being saturated cycles considered as a subclass of subcritical ones with no vapor superheating, and the employment of the recuperator can be optionally activated. The ORC optimization procedure aims at minimize/maximize a selected objective function by varying a certain number of design variables. In this research work, the selected objective function is the ORC plant system efficiency, which is proportional to the net power output and can be expressed as the product of cycle thermodynamic efficiency and heat recovery factor, as reported in Equation 1. However, the model can be easily adapted for more complex analyses as technoeconomic (minimization of system specific cost or levelized cost of electricity) and multi-objective optimizations.

$$ObjFunc.: \quad W_{el} = W_{gen} - W_{pump} - W_{fan}\,, \tag{1a}$$

$$ObjFunc.: \quad \eta_{system} = \eta_{cycle}\chi_{recovery} = \frac{W_{el}}{Q_{in}}\frac{Q_{in}}{Q_{in,max}} \tag{1b}$$

Four DVs are selected: (i) condensation temperature, cycle (ii) maximum pressure and (iii) maximum temperature and (iv) recuperator pinch point temperature difference. All the other plant quantities for the complete cycle definition are reported in Table 1 and kept constant during the plant optimization procedure. Among them, the turbine efficiency can be set equal to a fixed value or calculated as function of other cycle parameters by means of the performance map described in Section 3.3, in order to have a clear link between cycle DVs and expander performance. Some constraints are considered in the optimization procedure, among which the most limiting are: avoidance of two-phase flow expansion (i.e. vapor quality larger than one at the turbine outlet), and a maximum expansion ratio equal to 60 in order to avoid unfeasible single-stage turbine designs. ORC is condensed in a direct dry air-cooled heat exchanger having a design analogous to engine radiator: nominal air ambient temperature is equal to 25°C. A high-rotational speed generator is considered in order to allow for effective turbine efficiency optimizations avoiding the use of gearbox. The optimization routine includes a global gradient-free optimization procedure implementing a self-adaptive Differential Evolution algorithm and a local one exploiting SLSQP, a sequential quadratic programming (SQP) algorithm for nonlinearly constrained gradient-based optimizations.

ΔT heat exchangers		Heat exchangers pressure drops	
$\Delta T_{pp,PRHE}$, °C	10	ΔT_{cond}, °C	0.5
$\Delta T_{pp,cond}$, °C	2	ΔP_{desh}, %	0.02
Components efficiency		ΔP_{eco} (sub), bar	0.5
η_{pump}	0.5	ΔT_{eva} (sub), °C	1
η_{turb}	Fixed or Calculated	ΔP_{sh} (sub), bar	0.5
$\eta_{el,mecc,gen}$	0.98	ΔP_{PRHE} (sup), bar	1
$\eta_{el,mecc,pump}$	0.98	ΔP_{rec} (sup), %	0.002
η_{fan}	0.7	ΔP_{air}, mbar	22

Table 1: ORC model assumptions.

2.2 RIT reduce-order model description

The comprehensive reduced-order model developed, named RITML, implements several features that make it a flexible tool to carry out a preliminary design of single-stage radial inflow turbines, especially tailored for machines operating with organic fluid and for small-power high-temperature applications. In this section the main features are presented but its detailed description, together with a rigorous validation strategy, may be found in a paper recently published (Manfredi et al.).

The mean-line method, i.e. a low-fidelity approach based on the solution of 1D continuity, energy, and momentum equations, alongside loss correlations, includes the design of the nozzle, either of converging or converging-diverging type, the vaneless interspace, the rotor, with either radial or backswept blades at the inlet, and, eventually, of a downstream conical diffuser. An independent routine for each component is sequentially solved by the code, leading to a flexible and modular design procedure. To properly take into account the loss generation mechanisms across each component, a suitable set of empirical models was selected through a loss sensitivity analysis, whose details can be found in (Manfredi et al.) together with the set of loss correlations employed. The mandatory parameters required as inputs by the method to carry out the design are the inlet conditions, namely the total inlet pressure, and temperature, the flow angle at the nozzle inlet, the mass flow rate, and the required pressure ratio. In addition to the inputs, other parameters, also referred to as design variables (DVs), which include several geometrical parameters and the rotor rotational speed, are required to solve the flow field at each turbine station. The method implements a strategy to handle nozzle choking conditions and three different geometries may be contemporary investigated: converging subsonic nozzles, converging ones in chocking conditions with post-expansion, and supersonic converging-diverging geometries. However, the analyses and the turbine design procedures carried out in the present work are limited to converging-diverging nozzle, since the large Vr values involved correspond to high pressure ratios through the machine that in turn lead to supersonic Mach numbers at the stator outlet, for which a converging-diverging nozzle architecture results more efficient. The model retrieves the full turbine geometry, comprehensive of nozzle/rotor blade angles, clearances, blade thicknesses, cascade pitches, chords and openings, evaluates the average flow quantities and thermodynamic state at each turbine section, and estimates its performance, as proved by the extensive validation procedure against the performance data of 7 radial turbines, reported in (Manfredi et al.).

The DVs can be optimized in order to maximize turbine total-to-static efficiency, exploiting an outer algorithm to be coupled with RITML. In particular, the same optimization routine described at the end of Section 2.1 is implemented, which involves both gradient-free global and nonlinearly-constrained gradient-based local optimization procedures. The number and kind of DVs to be included in the optimization problem may be freely set by the user, making the code flexible and suitable for multi-level design strategies. Table 2 lists the parameters considered as DVs for such procedures and the corresponding ranges of variation, which define the design space investigated by the optimization algorithms. In Table 2 the subscripts 3, 4, 6 refer to nozzle outlet, rotor inlet and rotor outlet respectively. $\beta_{e,PE}$ is

DVs	Variation Ranges	DVs	Variation Ranges
ω_s	0.7-1.3	$\beta_{e,PE}$	0.9-1.1
α_3, deg	70-81	$r_{6,hub}$, m	0.006-0.1
$r_{6,hub}/r_{6,sh}$	0.1-0.7	$r_4/r_{6,sh}$	1.15-1.5
r_3/r_4	1.005-1.1	r_1/r_3	1.1-1.5
b_4/D_4	0.03-0.09	L_z/r_4	1.1-1.5

Table 2: Optimization procedure DVs and corresponding variation ranges.

the post-expansion/post-compression pressure ratio, defined as the ratio between the pressure at the inlet of the semi-bladed region over the one at the nozzle outlet (i.e. at radius r_3), and defines the degree of under-expansion/over-expansion in supersonic nozzles. Several constraints are considered in the present analysis to supervise those parameters which are not directly optimized and to avoid non-physical solutions. It is worthwhile to highlight that the lower limit of each physical dimension of the turbine was constrained to a certain minimum value (e.g. rotor hub radius > 6 mm, rotor axial length > 5 mm, stator heights and rotor inlet height > 2 mm, trailing edge > 0.15 – 0.25 mm for stator and rotor respectively, axial, radial and backplate clearance > 0.1 mm, nozzle radial chord > 5 mm) to ensure the feasibility of the final proposed geometry. Other constraints concern the flow field, such as for example the maximum Mach number at the nozzle outlet (< 2.5), the maximum flow turning within the rotor (< 120°), or the maximum Mach number at the rotor inelt/outlet (< 1).

3. PRELIMINARY ANALYSIS AND TURBINE MAP DEFINITION

3.1 Preliminary considerations on ORC design

The ORC numerical code has been adopted for a preliminary analysis in which several hundreds of cycles are designed considering different constant turbine efficiency values. The objective of such analyses is to retrieve useful ranges of SP and Vr to set as bounds for the development of the expander maximum efficiency map. Both recuperative ($\Delta T_{pp,rec}$ = 2°C) and non-recuperative cycles are investigated while three turbine efficiency values are adopted, namely 70%, 80% and 90%. The others three design variables defined in Section 2.1 are varied in the following ranges in order to cover the whole design space for the ORC cycle:

- *Cycle maximum pressure*. Both subcritical and supercritical cycles are investigated in the range between 7.4 bar, corresponding to a low evaporating temperature of 85°C, and 107.2 bar, corresponding to 3 times the critical pressure;
- *Cycle condensation temperature*. Minimum value (29°C) corresponds to very small pinch point temperature difference and wide heat transfer area condenser and implies a minimum pressure of 1.5 bar, compatible with the avoidance of non-condensable gases leakage. Maximum value (80°C) is selected in order to investigate also supercritical cycles with non-excessive pressure ratio;
- *Turbine inlet temperature*. Minimum value coincides with saturated condition for medium-low evaporation temperature subcritical cycles while it is affected by the constraint of single-phase flow expansion for high pressure subcritical and supercritical cycles. Maximum value is defined by fluid thermal stability temperature.

Optimal design of the six cycles is reported in Table 3. It is of interest to note that all the optimal configurations are supercritical, adopt a similar condensation temperature, which is higher than the lower bound, and push the turbine inlet temperature up to the maximum value. Optimal cycle efficiency is strongly affected by turbine efficiency while working fluid mass flow rate is mainly affected by the presence of the recuperator. These results also prove that a sensitivity analysis on turbine efficiency is not the correct approach to optimize an ORC power plant: optimal cycle design parameters are slightly affected by turbine assumed efficiency and the higher is the efficiency the higher is the turbine Vr, which is unrealistic when a single-stage turbine is adopted. Figure 1.a depicts the maximum system efficiency

Cycle	Non Recuperative			Recuperative ($\Delta T_{pp,rec}$=2°C)		
η_{turb}	70%	80%	90 %	70%	80%	90 %
Case	A	B	C	D	E	F
T_{cond}, °C	38.5	37.7	37.2	36.6	36.1	35.4
P_{max}, bar	57	60.2	62.7	53.6	56.0	58.7
T_{inT}, °C	240	240	240	240	240	240
η	12.6	15.0	17.4	15.0	17.8	20.6
W_{el}, kW	6.8	8.1	9.4	8.1	9.6	11.1
$\dot{m}_{ORC}$, g/s	169.6	171.4	172.9	201.0	201.6	201.6
SP, mm	8.2	8.3	8.4	9.1	9.2	9.2
Vr	30.7	33.7	36.1	29.0	31.8	34.2

Table 3: Optimal cycle results for the six investigated plants in the preliminary analysis.

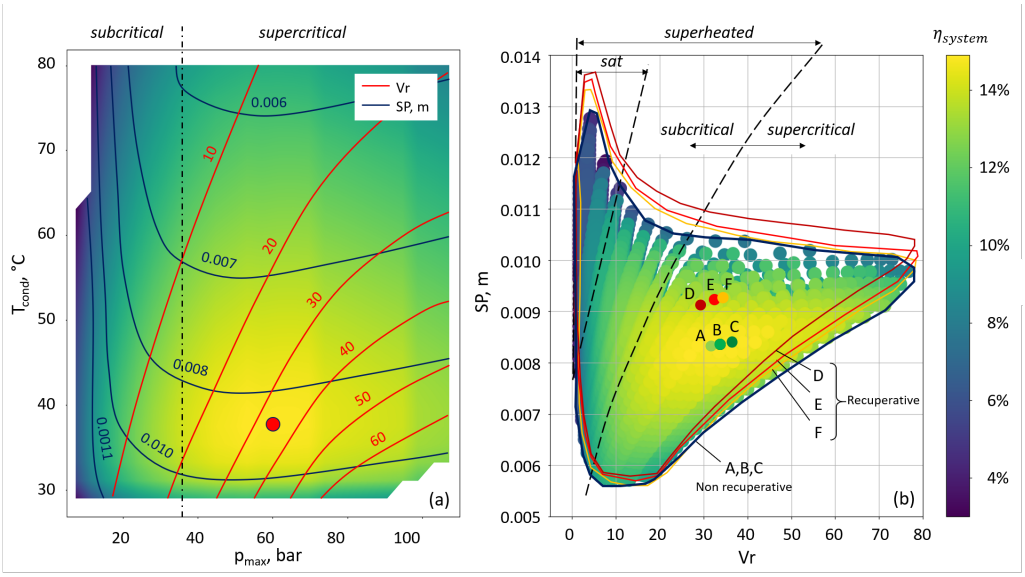

Figure 1: Graphical results for Case B: (a) maximum cycle efficiency, SP and Vr isolines as function of cycle maximum pressure and condensation temperature at optimal turbine inlet temperature (b) maximum cycle efficiency reported on turbine SP and Vr map, plus envelope of SP and Vr for the different investigated cycles (lines) and location of optimal designs (markers).

as function of condensation temperature and maximum pressure always at the optimal cycle maximum temperature for a non-recuperative cycle with 80% turbine efficiency (case B of Table 3). Contours of iso-SP and iso-Vr are also reported together with the optimal design point (red dot). It is possible to underline that the region of maximum efficiency is extremely wide and extends up to very high cycle maximum pressure and pretty high condensation temperatures, corresponding to intermediate values of both SP ($0.007 < SP < 0.009$) and Vr ($15 < Vr < 55$). Figure 1.b depicts the system efficiency as function of turbine SP and Vr for case B and concurrently delimits the ranges of SP and Vr for the other cases, reporting the corresponding envelopes (colored lines). Finally, marker locations define the optimal solution for each case reported in Table 3. Results clearly highlight that the envelops of Vr and SP are quite overlapped and they are thus not particularly affected by both the adoption of recuperator and the actual value of turbine efficiency. This suggests that the choice of Vr and SP ranges based on the envelopes reported in Figure 1.b is appropriate and would lead to a turbine performance map definition that can be used during the cycle optimization independently of the cycle architecture.

Parameter	Turbine X	Turbine Y	Turbine K	Turbine W
T_{in} - p_{in}, °C - bar	130.3, 19.2	205.9, 22.8	213.4, 45	192.5, 50
$T_{out,is}$ - p_{out} , °C - bar	51.3, 1.6	127.7, 1.6	121.8, 3.8	87.8, 5.8
m_{ORC}, g/s	219.9	205.1	471.3	681.6
Z_{in} - Z_{out}	0.66, 0.95	0.82, 0.98	0.63, 0.94	0.41, 0.87
V_{in} - V_{out}, m^3/s	0.0019, 0.027	0.0023, 0.0319	0.002, 0.0287	0.0016, 0.0232
η_{turb}, %	88.5	87.7	88.9	89.6
Nozzle				
D_{in} - D_{out}, mm	48, 36	46.6, 34.6	46.7, 34.7	47.5, 35.5
h_{in} -h_{out}, mm	2.1, 2.1	2.1, 2.1	2.1, 2.1	2.2, 2.2
Rotor				
ω_s - ω, kRPM	1.03, 103	1.09,130	1.06,114	1.03, 90
D_{in} - D_{out}, mm	34.6, 23	33.3, 22.3	33.4, 22.3	34.1, 22.6
h_{in} - h_{out}, mm	2, 7.7	2, 7.1	2, 7.1	2.1, 7.4

Table 4: Analysis over four RITs with the same SP (0.011 m) and Vr (14) but characterized by different expansion inlet and outlet conditions and compressibility factors. Results are obtained optimizing the turbines with RITML.

3.2 Similarity theory consistency check

In order to check the consistency of adopting SP and Vr as independent parameters for the turbine analyses, four RITs with the same SP (0.011 m) and Vr (14) but characterized by different expansion inlet and outlet conditions and compressibility factors are optimized adopting RITML code, as summarized in Table 4. Turbine X expands from saturated conditions, turbine Y is representative of a superheated subcritical cycle while turbines K and W expand from supercritical region. It is possible to note that not only the non-dimensional parameters but also the physical geometric dimensions of the four turbines are rather similar, being all of them characterized by the same SP. Although the rotational speed is quite different, the corresponding specific speed ω_s is similar for all the cases. Moreover, the four turbines exhibit very similar efficiencies that lie in an interval ranging between ±1% with respect to the average value of 88.7%. This deviation is within the range of accuracy claimed by the adopted mean line method. This example supports the choice of adopting SP and Vr as independent similarity theory parameters for the turbine map definition.

3.3 Turbine maximum efficiency map definition

single-stage radial inflow turbine maximum efficiency map is defined by optimizing 12 different turbines (markers in Figure 2.a) covering most of the region of possible SP and Vr values obtained through the preliminary analysis previously carried out. Figure 2.b depicts the maximum attainable turbine efficiency against the specific speed for the three designs enumerated in Figure 2.a. Additionally, Figure 2.c reports the loss breakdown for six turbine designs, those connected by a dashed black line in Figure 2.a. This allows to investigated the effect of the Vr for a fixed value of the SP and of the SP for a fixed Vr on the variation of the different loss contributions. The following observations can be reported:

- Turbine SP and Vr strongly affect turbine maximum efficiency which cannot be assumed constant in the whole design space. Calculated values range between 77% and 90% but lower efficiency is expected for Vr higher than 50 and SP lower than 0.007 m;
- Rotational speed has a large impact on turbine performance and must be carefully optimized. Optimal specific speed value depends on the SP and Vr but this analysis confirms that a good first attempt value of ω_s is around 1, as also suggested by (Perdichizzi and Lozza, 1987);
- An increment of Vr leads to an efficiency penalization mainly due to an increase of stator passage loss contribution. In fact, higher Vr values lead to lower pressure levels at the nozzle outlet, which in turn imply larger Mach number values and, consequently, higher losses associated with blade

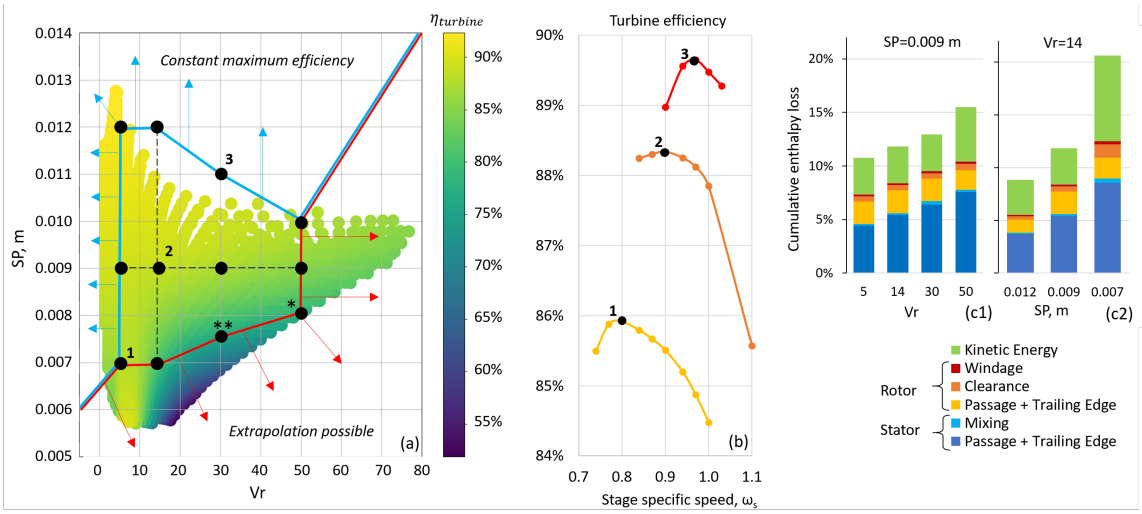

Figure 2: (a) turbine maximum efficiency as function of SP and Vr, markers are the turbines optimized with RITML mean line code. (b) variation of turbine efficiency for markers 1-2-3 as function of turbine ω_s (c) enthalpy loss breakdown for (left) turbines with the same SP (0.009m) and different Vr (5-50) and (right) turbines with same Vr (14) and different SP (0.007m-0.012m).

boundary layers development. Performance penalization is more marked at smaller SP;

- A reduction of SP produces a pronounced increase of the nozzle passage loss contribution. A possible explanation of this effect is likely to be ascribed to the geometry dimensions reduction that results decreasing the SP value. In fact, the turbine size shrinking is limited by the constraints previously mentioned concerning the minimum values of main geometrical parameters. Therefore, to reach the desired pressure level at the nozzle outlet, mainly affected by the expansion ratio Vr, the optimizer is forced to rise the nozzle outlet angle value, leading an increase of the flow wetted surface and in turn of the friction loss contribution. The increment of clearance losses for lower SP values is to be ascribed to the increase of axial and radial gap relative size occurring when the geometry is shrunk;
- To develop the map the rotational speed has not been limited. As result, values of rotational speed close to 200000 RPM have been found for turbine labelled with * in Figure 2.a, a strong efficiency penalization is expected for machines in this region if maximum shaft rotational speed is constrained to lower values because of bearings, lubrification and frequency conversion issues.

Efficiency results have been interpolated with a best fit correlation having a corrected R^2 equal to 0.98, average absolute error equal to 0.12% and maximum error equal to +0.35% for turbine labelled with ** in Figure 2.a. The interpolating relation can be extrapolated for lower SP and Vr higher than 50 but it likely results in turbine performance overestimation. On the contrary, considering the pretty flat trend approaching high SP and small Vr extrapolation out of this region is not suggested because of non-physical behavior of the fitting function. In these cases it is simply suggested to keep the maximum efficiency value obtained at the closer point on the map boundary, which however would result in a slight underestimation of turbine performance.

4. ORC COMPREHENSIVE DESIGN

Turbine performance map is implemented in the ORC optimization tool. Figure 3.a depicts the maximum cycle efficiency map retrieved for the non-recuperative cycle configuration and by adopting the turbine efficiency correlation. This figure is to be compared against the corresponding map of Figure 1.a, obtained for a constant turbine efficiency equal to 80%. It is possible to highlight the tradeoff between maximizing cycle theoretical performance (attainable with an isentropic turbine and analogous to the

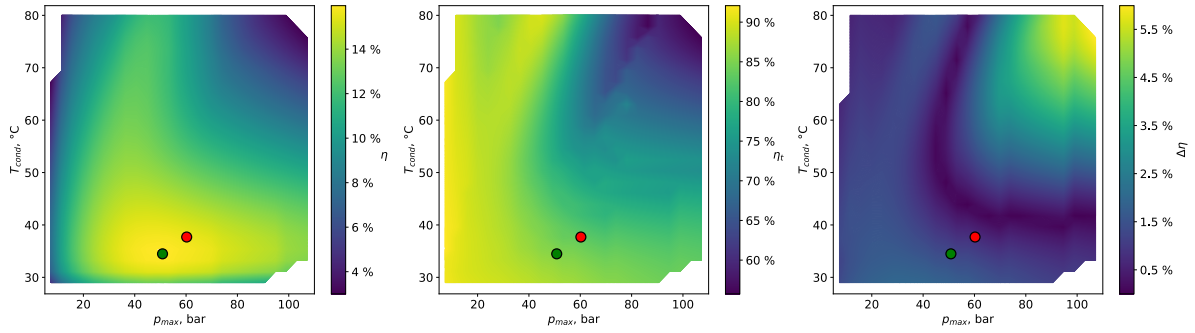

Figure 3: Comprehensive analysis results for the non-recuperative case. (a) cycle efficiency as function of maximum pressure, condensation temperature at optimized turbine inlet temperature, (b) turbine efficiency for the optimal cycles, (c) difference between cycle efficiency of finalized and preliminary results. Red marker is the optimal design point with 80% constant turbine efficiency while green one corresponds to the ORC optimization with turbine map implemented.

cases with fixed turbine efficiency) and the need of maximizing turbine performance, whose efficiency is reported in Figure 3.b in function of condensation temperature and cycle maximum pressure.As evidenced by Figure 3.a, the analysis catches the negative effect of simultaneously adopting high condensation temperature and high maximum pressures: these conditions strongly penalize the turbine efficiency due to SP reduction. On the contrary, the lower is the maximum pressure and the condensing temperature the higher is the turbine performance. Optimal design reflects these considerations and adopts a turbine inlet pressure lower than all the previous cases (50.83 bar), a lower Vr (29.46) and a larger SP (0.00859 m). The difference between the cycle performance calculated with turbine efficiency correlation and the case with fixed turbine efficiency equal to 80% (refer to Figure 1.a) is reported in Figure 3.c. It is interesting to note that in most of the design space the difference is limited to around 1.2%-1.8% points of efficiency that corresponds to a relative difference of around 10%, a difference that would be enlarged if a different constant value of turbine efficiency is assumed. Figure 3 also highlights the shifting of the optimal design point in the two cases (from the red dot to the green one). Similar observations are valid also for the recuperative cycle. Optimal recuperative and non-recuperative cycle results obtained with turbine efficiency correlation are reported in Table 5.

A final example is also proposed in Table 5 for an engine of a smaller size by simply reducing the exhaust mass flow rate down to 0.134 kg/s (-33%), still considering non-recuperative cycle configuration. If the design point is kept the same obtained with the fixed turbine efficiency analysis the lower organic fluid mass flow rate would result in a lower SP and consequently in a very low turbine efficiency value. In this case the optimization algorithm reduces the maximum pressure in order to reduce the turbine enthalpy drop, increasing the turbine SP by concurrently reducing the Vr. Final cycle is subcritical (29 bar) superheated with an optimal turbine inlet temperature considerably lower than the maximum value (208°C). Figure 4 compares the Ts diagrams for the three optimal non recuperative cycles: the one resulting from a constant turbine efficiency (80%), which represents the term of comparison, and the two cycles obtained exploiting the turbine performance map (characterized by exhaust mass flow of 0.2 kg/s and 0.134 kg/s respectively).

5. CONCLUSIONS

The outcomes of this research study can be classified in two different topics:

- From the point of view of system optimization, it is possible to underline that the implementation of a map for expected turbine performance allows to guide the optimization algorithm towards solution which are more representative of the correct optimal design of the system. The adoption of a proper turbine map allows in the investigated case to design the system with lower maximum pressures, leading to a gain in performance. Differences are particularly marked in the lower size

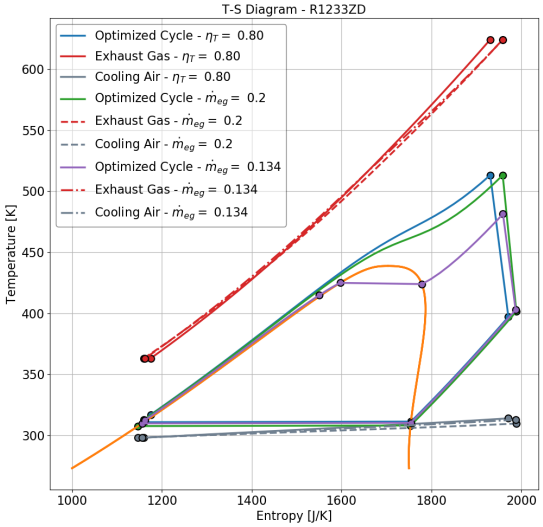

Figure 4: Temperature-specific entropy diagram for: the optimal non recuperative cycle with fixed turbine 80%, the two optimal non recuperative cycles adopting the turbine map with nominal and reduced exhaust mass flow rate.

Case	Non Rec	Rec	Non Rec (-33%)
T_{cond},°C	34.5	34.5	36.7
p_{max}, bar	50.8	53.0	27.7
T_{max}, °C	240	240	208.1
$\Delta T_{pp,rec}$, °C	-	2	-
η_{system}, %	16.0	20.0	13.6
$\dot{W}_{el}$, kW	8.6	10.8	4.9
m_{ORC}, g/s	163.0	197.6	113.7
SP, mm	8.6	9.3	7.3
VR	29.5	30.6	13.6
η_{turb}, %	85.2	88.1	82.7

Table 5: Optimal results for the non-recuperative and the recuperative cycle adopting turbine performance map and results for both normal and reduced size (-33%) engine.

example where the optimal cycle becomes subcritical. Future steps of this work will be focused on the analyses for other working fluids. In particular, the benefit in introducing a map for turbine efficiency would be even more marked for high-critical temperature working fluids which are generally characterized by high Vr and large SP with a non trivial effect on turbine performance;

- From the point of view of the study of small radial expanders, it is possible to highlight that the choice of Vr and SP as independent parameters is a proper choice that allows to define a performance map that can be used with sufficient accuracy (±1%, as demonstrated in Section 3.2, plus the intrinsic prediction uncertainty of the mean-line model), independently on the specific value of pressure ratio, inlet compressibility factor and fluid mass flow rate. Next steps will deal with a more extensive exploration of the ranges of SP and Vr in order to improve map accuracy and with the extension of the validation to other working fluids in order to obtain a very general fluid-independent turbine performance map.

ACKNOWLEDGEMENT

This research is part of the *Energy for Motion* project of the Department of Energy of Politecnico di Milano, funded by the Italian Ministry of University and Research (MUR) through the *Department of Excellence* grant 2018-2022.

REFERENCES

Marco Astolfi and Ennio Macchi. Efficiency correlations for axial flow turbines working with non-conventional fluids. In *3rd International Seminar on ORC Power Systems*, pages 12–14, 2015.

AH Bademlioglu, AS Canbolat, N Yamankaradeniz, and O Kaynakli. Investigation of parameters affecting organic rankine cycle efficiency by using taguchi and anova methods. *Applied Thermal Engineering*, 145:221–228, 2018.

Sebastian Bahamonde, Matteo Pini, Carlo De Servi, Antonio Rubino, and Piero Colonna. Method for the preliminary fluid dynamic design of high-temperature mini-organic rankine cycle turbines. *Journal of Engineering for Gas Turbines and Power*, 139(8), 2017.

Ian H. Bell, Jorrit Wronski, Sylvain Quoilin, and Vincent Lemort. Pure and pseudo-pure fluid thermophysical property evaluation and the open-source thermophysical property library coolprop. *Industrial & Engineering Chemistry Research*, 53(6):2498–2508, 2014. doi: 10.1021/ie4033999.

Piero Colonna, Emiliano Casati, Carsten Trapp, Tiemo Mathijssen, Jaakko Larjola, Teemu Turunen-Saaresti, and Antti Uusitalo. Organic Rankine Cycle Power Systems: From the Concept to Current Technology, Applications, and an Outlook to the Future. *Journal of Engineering for Gas Turbines and Power*, 137(10), October 2015. ISSN 0742-4795. doi: 10.1115/1.4029884.

European FluoroCarbons Technical Committee. Hcfo-1233zd(e) chillers receive environment awards around the world. `http://precog.iiitd.edu.in/people/anupama`, January 2020.

Luca Da Lio, Giovanni Manente, and Andrea Lazzaretto. A mean-line model to predict the design efficiency of radial inflow turbines in organic rankine cycle (orc) systems. *Applied Energy*, 205:187–209, 2017.

V Dolz, R Novella, A García, and J Sánchez. Hd diesel engine equipped with a bottoming rankine cycle as a waste heat recovery system. part 1: Study and analysis of the waste heat energy. *Applied Thermal Engineering*, 36:269–278, 2012.

A. Perdichizzi E. Macchi. Efficiency prediction for axial flow turbines operating with non-conventional working fluids. *J. of Eng. for Power*, 103:712–724, October 1981.

Michael Glensvig, Heimo Schreier, Mauro Tizianel, Helmut Theissl, Peter Krähenbühl, Fabio Cococcetta, and Ivan Calaon. Testing of a long haul demonstrator vehicle with a waste heat recovery system on public road. Technical report, SAE Technical Paper, 2016.

E. W. Lemmon, , Ian H. Bell, M. L. Huber, and M. O. McLinden. NIST Standard Reference Database 23: Reference Fluid Thermodynamic and Transport Properties-REFPROP, Version 10.0, National Institute of Standards and Technology, 2018. URL `https://www.nist.gov/srd/refprop`.

Marco Manfredi, Marco Alberio, Marco Astolfi, and Andrea Spinelli. A reduced-order model for the preliminary design of small-scale radial inflow turbines. In *Still to be published*.

Massimo Masi, Luca Da Lio, and Andrea Lazzaretto. An insight into the similarity approach to predict the maximum efficiency of organic rankine cycle turbines. *Energy*, 198:117278, 2020.

Andrea Meroni, Jesper Graa Andreasen, Giacomo Persico, and Fredrik Haglind. Optimization of organic rankine cycle power systems considering multistage axial turbine design. *Applied Energy*, 209:339–354, 2018.

Antonio Perdichizzi and Giovanni Lozza. Design criteria and efficiency prediction for radial inflow turbines. In *ASME 1987 International Gas Turbine Conference and Exhibition*. American Society of Mechanical Engineers Digital Collection, 1987.

G. Persico and M. Pini. Fluid dynamic design of organic rankine cycle turbines. In *Organic Rankine Cycle (ORC) Power Systems*, pages 253–297. Elsevier, 2017. doi: 10.1016/b978-0-08-100510-1.00008-9.

Thomas Tartière and Marco Astolfi. A world overview of the organic rankine cycle market. *Energy Procedia*, 129:2–9, 2017.

Martin T White and Abdulnaser I Sayma. Simultaneous cycle optimization and fluid selection for orc systems accounting for the effect of the operating conditions on turbine efficiency. *Frontiers in Energy Research*, 7:50, 2019.

Kangyi Yang, Michael Bargende, and Michael Grill. Evaluation of engine-related restrictions for the global efficiency by using a rankine cycle-based waste heat recovery system on heavy duty truck by means of 1d-simulation. Technical report, SAE Technical Paper, 2018.